THE JOURNAL OF PHYSICAL CHEMISTRY A

Article

pubs.acs.org/JPCA

Guest Inclusion in Cucurbiturils Studied by ESR and DFT: The Case of Nitroxide Radicals and Spin Adducts of DMPO and MNP

Mariana Spulber,[†,‡] Shulamith Schlick,*[,†] and Frederick A. Villamena[§]

[†]Department of Chemistry and Biochemistry, University of Detroit Mercy, 4001 West McNichols, Detroit, Michigan 48221, United States

[§]Department of Pharmacology and Center for Biomedical EPR Spectroscopy and Imaging, The Davis Heart and Lung Research Institute, College of Medicine, The Ohio State University, Columbus, Ohio 43210, United States

Supporting Information

ABSTRACT: We present an ESR and DFT study of the interaction of cucurbiturils CB[6], CB[7], and CB[8] with di-*tert*-butyl nitroxide ($((CH_3)_3C)_2NO$ (DTBN) and with spin adducts of 5,5-dimethyl-1-pyrroline-*N*-oxide (DMPO) and 2-methyl-2-nitrosopropane (MNP). The primary goal was to understand the structural parameters that determine the inclusion mechanism in the CBs using DTBN, a nitroxide with great sensitivity to the local environment. In addition, we focused on the interactions with CBs of the spin adducts DMPO/OH and MNP/CH_2COOH generated in aqueous CH_3COOH. A *range* of interactions between DTBN and CBs was identified for pH 3.2, 7, and 10. No complexation of DTBN with CB[6] was deduced in this pH range. The interaction between DTBN and CB[7] is evident at all pH values: "in" and "out" nitroxides, with ^{14}N hyperfine splitting, a_N, values of 15.5 and 17.1 G, respectively, were detected by ESR. Interaction of DTBN with CB[8] was also detected for all pH values, and the only species had a_N = 16.4 G, a result that can be rationalized by an "in" nitroxide in a less hydrophobic environment compared to CB[7]. Computational studies indicated that the DTBN complex with CB[7] is thermodynamically favored compared to that in CB[8]; the orientations of the NO group are parallel to the CB[7] plane and perpendicular to the CB[8] plane (pointing toward the annulus). Addition of sodium ions led to the ESR detection of a three-component complex between CB[7], DTBN, and the cations; the ternary complex was not detected for CB[8]. The DMPO/OH spin adduct was stabilized in the presence of CB[7], but the effect on a_N was negligible, indicating that the N−O group is located *outside* the CB cavity. Computational studies indicated more favorable energetics of complexation for DMPO/OH in CB[7] compared to DTBN. An increase of a_N was detected in the presence of CB[7] for the MNP/CH_2COOH adduct generated in CH_3COOH, a result that was assigned to the generation of the three-component radical between the spin adduct, sodium cations, and CB[7].

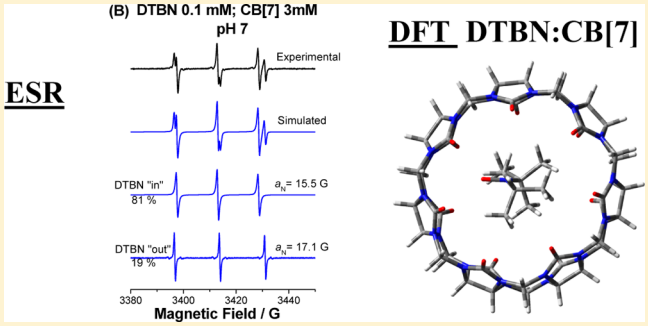

INTRODUCTION

Cucurbiturils (CBs) are macrocyclic cavitands that have attracted increased interest in recent years, due to their ability to form inclusion compounds with guest molecules. As shown in Figure 1, CBs consist of glycoluril units linked by methylene bridges, and their name expresses the shape similarity with the pumpkin family (Cucurbitaceae).[1,2] CBs have highly symmetrical structures with two identical portal ends flanked by carbonyl groups and an inner hydrophobic cavity whose size depends on the number of glycoluril units.[1−5] The study of CBs has been encouraged by the recent commercial availability of CBs with n = 5−8.

In terms of cavity size, CB[6], CB[7], and CB[8], with 6, 7, and 8 glycoluril units, respectively, can be compared with α-, β-, and γ-cyclodextrin: The inner diameter of the hydrophobic cavity of CB[6] is 5.8 Å (compared to 5.7 Å for α-cyclodextrin, α-CD), allowing it to accommodate small guests, and the portals formed by the carbonyl groups, with diameter of 3.9 Å, can bind cations; CB[7] has an inner diameter of 7.3 Å (7.8 Å for β-CD) and a portal diameter of 5.4 Å; and CB[8] has an inner diameter of 8.8 Å (9.5 Å for γ-CD) and a portal diameter of 6.9 Å.[6−8] Although the size similarities are obvious, CDs and CBs exhibit different binding properties: CBs possess an equatorial symmetry plane that makes the two openings identical; in CDs they are different, the smaller opening lined by primary hydroxyl groups and the larger one lined by twice as many secondary hydroxyl groups.[9] Due to their structures, intermolecular interactions between CBs or cyclodextrins (CDs) and guest molecules are also different. In the case of CDs, the hydrophobic interactions are primarily responsible for guest inclusion, whereas in CBs *two* types of intermolecular forces are operative: ion−dipole between cationic guests and

Received: April 12, 2012
Revised: July 25, 2012
Published: July 25, 2012

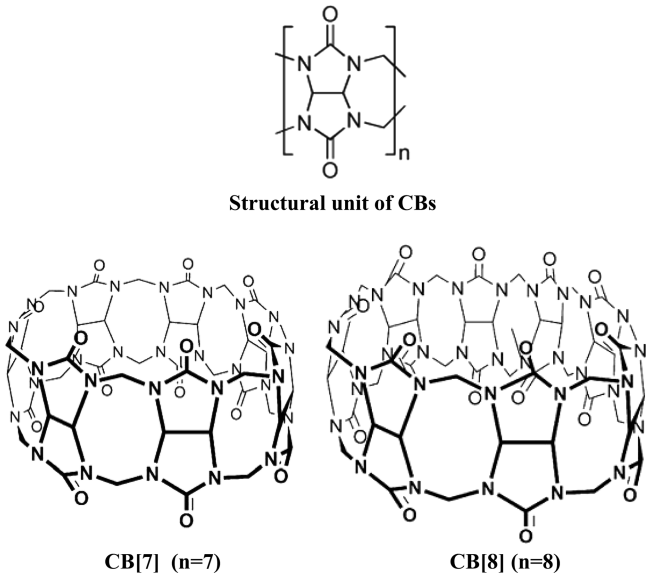

Figure 1. Structural unit of CBs (top) and CB[7] and CB[8] (below).[5].

the carbonyl oxygens lining both openings, and hydrophobic interactions between the guest and the inner surface of the CB cavity.[1,10] The binding of hosts in cucurbiturils is therefore highly selective. Moreover, in aqueous solutions, CBs can also form 1:1 and 1:2 host−guest interactions with association constants higher than those reported for the CDs, often by several orders of magnitude.[11] An interesting recent paper described the preparation of polymer−gold nanocomposites held together by CB[8] ternary complexes.[12] Despite the growing interest in CBs, details are missing about the precise complexation mechanism with neutral guests.[13] Moreover, characterization of the resulting complexes is complicated by the ability of CBs to form dimers, trimers, and tetramers.[10]

The formation of host−guest molecular assemblies held together by noncovalent interactions is the focus of numerous studies. However host−guest complexes are dynamically labile; therefore, only select methods can be used for measuring the kinetics of association and dissociation processes.[14,15] NMR spectroscopy is a useful characterization method in the case of relatively slow (on an NMR scale) exchange between the free and the complexed guest.[16] Recent papers have demonstrated the ability of ESR spectroscopy to distinguish *different* signals from complexed ("in") and uncomplexed ("out") paramagnetic species in CD hosts.[17,18] These studies were performed on inclusion complexes of nitroxide radicals and spin adducts, and the detection of "in" and "out" species was based on the determination of the ^{14}N hyperfine splitting (hfs), a_N, of the nitroxide, which is a sensitive indicator of the local polarity. Additional criteria for determining inclusion of nitroxides inside hosts are the line widths, which are broader in the ESR spectra of in nitroxides, and the line shapes, which reflect their lower rotational rates and longer rotational correlation times, τ_r. The increased stability of short-lived guests such as spin adducts in the presence of CD hosts was interpreted in terms of a longer half-life, $\tau_{1/2}$, due to complexation.[18a]

The ESR approach has been recently applied to the study of complex formation in various CBs. Details on CB[7] and two nitroxides (2,2,6,6-tetramethyl piperidine-*N*-oxyl (TEMPO) and benzyl *tert*-butyl nitroxide (BTBN)) as guests have been presented, based on the detection of the "in" nitroxide (with smaller a_N than in neat water and higher a_N in the presence of alkali cations) and "out" species.[19a] Complexation of BTBN with CB[8] led to the detection of a seven-line spectrum which was assigned to the formation of a trinitroxide supraradical.[19b]

An important study described the complexation between TEMPO or 2,2,6,6 tetramethyl-4-methoxypiperidin-1-oxyl and CB[7] and CB[8] at pH 7.[20] In the presence of CB[7], the "out" nitroxides (with the same ^{14}N hyperfine splitting, a_N, as in neat water) and in nitroxides (with smaller a_N) of both probes were detected. This study also reported that TEMPO included in CB[7] is efficiently protected against reduction by ascorbate, a major in vivo reducing agent of nitroxides.

The complexation of CB[7] and CB[8] with cationic nitroxides at neutral pH was interpreted based on probe location close to the carbonyl groups.[21] The seven-line signal was recorded in the presence of CB[8], and spectra simulations suggested spin exchange between three nitroxide radicals.[21]

Details on the inclusion mechanism at the molecular level for CDs and CBs have been deduced from theoretical studies. Recent papers have indicated the importance of CD-complexed nitrones in the trapping of superoxide radicals and the importance of density functional theory (DFT) calculations for an understanding of their extraordinary stability.[22] The calculations described the geometry of inclusion with the nitroxide group toward the annulus as the significant factor for adduct stability, in agreement with experimental results.[22] DFT calculations have also been carried out to help assess the stability of complexes for various CBs with ferrocene and isoniazid and to deduce the orientation of the guest molecule inside the host during the encapsulation process.[23]

We present an ESR study of supramolecular association for CB[6], CB[7], and CB[8] with di-*tert*-butyl nitroxide ($((CH_3)_3C)_2NO$, DTBN). This nitroxide was chosen because of its high sensitivity to the polarity of the medium deduced in our study of the DTBN:β-CD[18a] and its size, smaller than BTBN or TEMPO, thus favoring specific CB inclusion. The complexation of DTBN was studied as a function of pH in the range 3−10 and in the presence of sodium cations. The complexation between CB[7] and various spin adducts of 5,5-dimethyl-1-pyrroline-*N*-oxide (DMPO) and 2-methyl-2-nitrosopropane (MNP) spin traps (Chart 1) at pH 7 was also

Chart 1. Spin Traps Used To Generate the DMPO/OH and MNP/CH_2COOH Spin Adducts

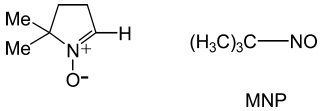

analyzed, and the results were compared with those published previously for β-CD.[18] The ESR results are complemented by DFT calculations of the stability and conformation of CB[7] and CB[8] complexes with DTBN and with the DMPO/OH adduct. To the best of our knowledge, we present the first ESR and DFT study of the interaction between CBs and *spin adducts*.

EXPERIMENTAL SECTION

1. Materials. DTBN, CB[6], CB[7], CB[8], and MNP were purchased from Sigma-Aldrich and used as received. High-purity DMPO was purchased from Enzo Life Sciences. Hydrogen peroxide, H_2O_2, was obtained from Sigma-Aldrich

dx.doi.org/10.1021/jp303536m | J. Phys. Chem. A 2012, 116, 8475−8483

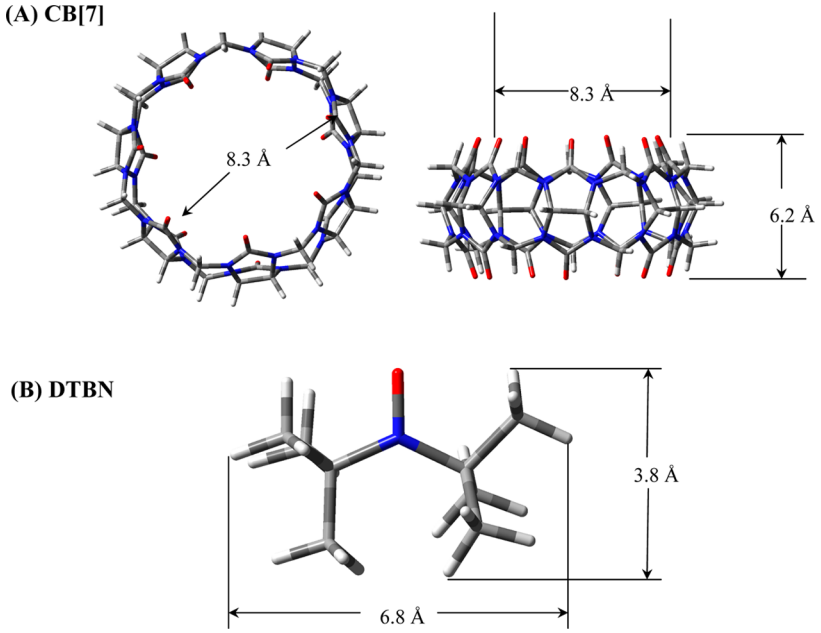

Figure 2. (A) Optimized geometries of CB[7] at the B3LYP/6-31G(d) level of theory. The diameters of DTBN parallel and perpendicular to the orientation of the N−O group are shown in (B).

as a 3% aqueous solution. Deionized "ultrapure" water with low conductivity and ≤10 ppb total organic carbon was provided by the Millipore Model Direct-Q UV system and used in the preparation of all aqueous samples.

2. Sample Preparation. Samples containing DTBN and CB[6], CB[7], or CB[8] were prepared by mixing a stock solution containing 0.1 mM DTBN and 12 mM CBs with the 0.1 mM DTBN solution, so that the final concentration of DTBN remained constant while the concentration of the CBs varied from 0.1 to 3 mM. The pH of the solution was 3.2. The pH of the stock solution was adjusted with a 2 M NaOH solution to the desired value (7 or 10); the samples were prepared in a similar way by diluting the stock solution with corresponding volumes of the DTBN solution, to a final constant concentration of DTBN. In order to see the effect of alkali cations, up to 2 mM NaCl was added to a 12 mM stock solution that was diluted with the DTBN solution so that the final concentration of DTBN remained the same.

The DMPO/OH spin adduct was obtained by mixing a 0.1 mL aqueous solution of the spin trap (1 mM DMPO) with 0.01 mL of 3% H_2O_2. The pH of each solution was adjusted to 7 with 2 M NaOH. The adduct of the carbon-centered radical adducts of MNP, MNP/CCR, was prepared by mixing a 0.1 mL aqueous solution of MNP (2×10^{-4} M) with 1 mL of acetic acid of concentration 2 M and 0.05 mL of 3% H_2O_2.[18] The pH of the solution was adjusted to 7 with NaOH. The spin adducts were generated, both in the absence (as control) and in the presence of CB[7] in increasing concentrations, by in situ UV irradiation of the appropriate solutions (with or without CB[7]) at 300 K in quartz capillary tubes placed inside the ESR resonator, using a 300 W ozone-free Xe arc equipped with a water filter (Oriel).

3. ESR Measurements. Spectra were recorded at 300 K using a Bruker X-band EMX spectrometer operating at 9.7 GHz with 100 kHz magnetic field modulation and equipped with the Acquisit 32 Bit WINEPR data system version 3.01 for acquisition and manipulation and the ESR 4111 VT variable temperature units. The microwave frequency was measured with the Hewlett-Packard 5350B microwave frequency counter. The hyperfine splittings (hfs) of the spin adducts were determined by simulating the spectra using the WinSim (NIEHS/NIH) package;[24] the simulation also determined the relative intensity of each component for spectra consisting of contributions from more than one spectral component. Typical acquisition parameters for all ESR spectra were the following: sweep width 100−150 G, microwave power 2 mW, time constant 20.48 ms, conversion time 41.94 ms, 2048 points, modulation amplitude 0.2−1 G, receiver gain 5×10^4, and 20−40 scans.

4. The Computational Procedure. The structures were chosen based on the most stable conformer/configurations using Spartan 04 at the MMFF level. All calculations were performed with Gaussian 03[25] at the Ohio Supercomputer Center. DFT calculations[26] at the B3LYP/6-31G(d) level of theory were used in this study to determine the optimized geometry of CB[7] and DTBN, and each yielded no imaginary vibrational frequency. A scaling factor of 0.9806 was used for the zero-point vibrational energy (ZPE) corrections in all the B3LYP/6-31G(d) geometries.[27] Negligible spin contamination of $0.75 < \langle S2 \rangle < 0.76$ was obtained for all the minima. Due to the size of the molecules, optimization of complexes involving CB[7], DMPO/OH, and DTBN were carried out at the HF/3-21G(d) level of theory, and gas phase bottom-of-the-well energies and spin densities were obtained from the natural population analysis (NPA) approach[28] using ONIOM two-layer calculations ONIOM(B3LYP/6-31G(d):HF/3-21G(d). The high layer contained the aminoxyl radical while the remaining atoms (i.e., CB[7]) formed the lower layer.

RESULTS AND DISCUSSION

We will start this section by presenting and discussing the complexation of DTBN by CBs; this section will include both ESR and DFT calculations. The second section includes results for the complexation of spin adducts of DMPO and MNP with the CBs and comparison of the results with reported data for some of these guests in the presence of CDs.

dx.doi.org/10.1021/jp303536m | J. Phys. Chem. A 2012, 116, 8475−8483

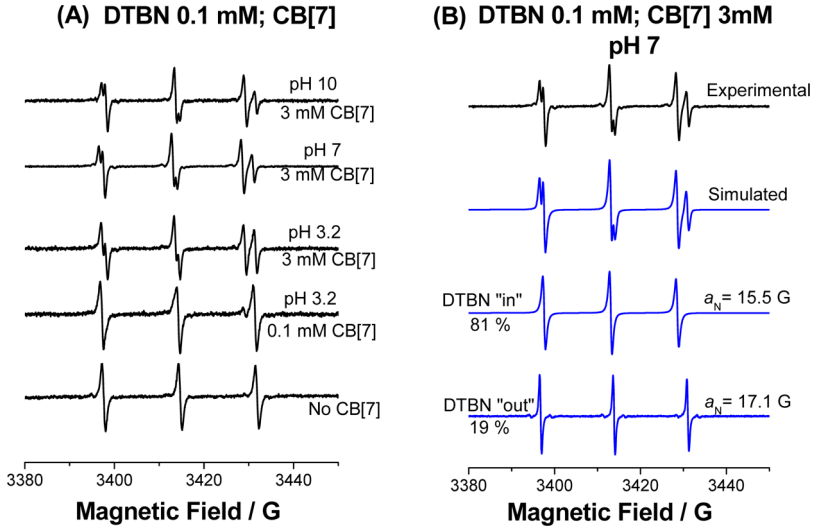

Figure 3. (A) ESR spectra at 300 K of DTBN in neat water, at the indicated pH and CB[7] concentrations. (B) Experimental and simulated ESR spectra of DTBN at pH = 7 and in the presence of 3 mM CB[7]. Experimental spectra are shown in black and simulated spectra in blue.

1. Complexation between DTBN and CBs. In aqueous solutions the ESR spectra of DTBN at 300 K reflect the ^{14}N hyperfine splitting a_N = 17.1 G and, depending on the ESR intensity, exhibit the typical ^{13}C satellites.[18a] Addition of CB[6] concentrations in the range 0.1−6 mM at pH = 7 and 10 (in order to increase the host solubility) showed no measurable changes in terms of a_N and line widths. The results are similar to those described in the case of DTBN with α-CD[18a] and can be explained by the lack of complexation, considering the smaller diameter of CB[6] (5.8 Å)[6−8] compared to DTBN (7 Å).[29]

The DTBN:CB[7] System. To set the stage for the computational part, we have used DFT to calculate the dimensions of CB[7] and DTBN: Figure 2 shows one of the two possible, and more plausible, conformations for CB[7], with the glycouril hydrogens oriented at the exterior of the molecule. The conformation gave an inner diameter of 8.3 Å. The calculated inner diameter for CB[7] is consistent with that previously observed using a computational approach and X-ray crystallography, 8.2 [30] and 7.3 Å,[7] respectively. The calculated inner diameter for CB[8] was 9.95 Å, close to computed value (10.33 Å)[30] and the value determined by X-ray (8.8 Å).[7] The predicted diameter for DTBN is 7 Å, as also reported in ref 29.

As shown in Figure 3A, addition of CB[7] to a 0.1 mM DTBN aqueous solution at 300 K results in the splitting of each of the three nitroxide ESR lines into two components with good resolution, an indication of the presence of "out" and "in" species; slow exchange on the ESR time scale is clearly seen. The two spectral components are detected for CB[7] concentrations of 0.1 and 3 mM and at pH = 3.2, 7, and 10. The in form exhibits distinctly lower a_N values, 15.5 G, compared to the corresponding out species, 17.1 G, as shown in Figure 3B for pH = 7 and CB[7] concentration of 3 mM. Moreover, the in a_N value (15.5 G) is significantly lower than that of DTBN in β-CD (16.6 G),[18a] indicating a more hydrophobic environment for DTBN within the CB[7] cavity. The a_N lowering, Δa_N, is 1.6 G, higher than that reported for TEMPO (0.9 G) and BTBN (1.2 G)[19a] in CB[7]; in ref 19a the "in" form is noticeable only by the splitting of the high-field line, compared to the splitting of all three lines shown in Figure 3B. Moreover, Δa_N is much higher than the values reported for the interaction reported with β-CD, which is 0.5 G.[18] The "in" a_N value is close to that for DTBN in lipids such as coconut oil[31] or corneum membranes,[32] a_N = 15.3 G, and indicates the high hydrophobicity of the CB[7] cavity. The strong effect on a_N also suggests that the nitroxide group in DTBN is deeply immersed in the CB[7] cavity. The relative intensity of the "in" form increases with CB[7] concentration from 0.1 to 3 mM at all three pH values studied (from 25% to 58% for pH 3.2 and to 81% at pH 7 and 10).

The magnitude of a_N depends not only on the local polarity but also on the conformation of the nitroxide. The dihedral angle, ϕ, is 2.4° in isolated DTBN, but higher, ϕ = 9.4°, for DTBN as guest in CB[7]. The dependence of the nitroxide a_N on conformation was proposed, where steric effects as well as hyperconjugation of the σ orbital with SOMO and/or formation of hydrogen bridges can contribute to the magnitude of the hyperfine splitting.[33] Franchi et al. proposed a similar effect on the conformation on the hyperfine splittings for nitroxides.[34] It is expected that hyperconjugation of SOMO with the C−Me σ-orbital would allow higher spin density on the N-atom, as shown computationally: ϕ = 2.4° vs 9.4°.

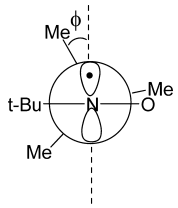

The DTBN:CB[8] System. Direct complexation in aqueous solutions between CB[8] and DTBN at pH 3.2, 7, and 10 is shown in Figure 4; only *one* form of DTBN is observed, with a_N = 16.4 G, higher than that observed for CB[7] as host (a_N = 15.5 G). Because only one nitroxide species was detected by ESR for the entire pH range (3.2−10) and in a wide range of CB[8] concentrations (0.1−3 mM), we tentatively rationalize the a_N value of 16.4 G as representing DTBN included in the host. The higher a_N value compared to CB[7] as host may be due to a less hydrophobic environment; however, a different conformation may also be possible in the larger CB[8] host.

dx.doi.org/10.1021/jp303536m | J. Phys. Chem. A 2012, 116, 8475−8483

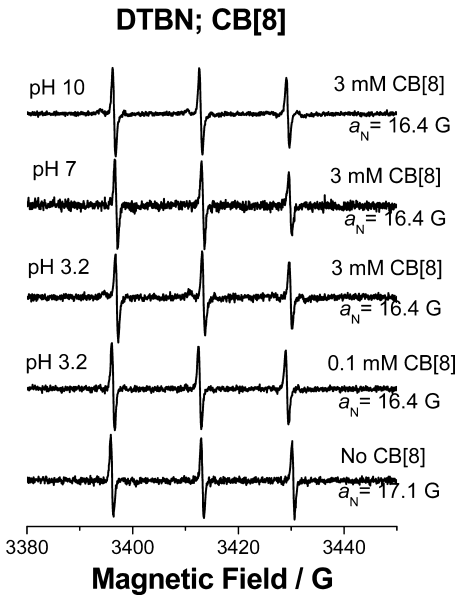

Figure 4. ESR spectra at 300 K of DTBN in neat water and in the presence of 0.1 or 3 mM CB[8], at the indicated pH values.

We note that this is the first reported CB[8] complexation with a neutral nitroxide in aqueous solution.

Complex formation between DTBN and CB[8] is supported by data depicted in Figure 5, which presents optimized complexes of CB[7] and CB[8] with DTBN at the HF/3-21G(d) level of theory. The closest aminoxyl−O to CB−O distances are 3.43 and 4.75 Å, respectively, and the bottom-of-the-well energies predicted for DTBN:CB[7] and DTBN:CB[8] are −13.0 and −10.6 kcal/mol, respectively. The aminoxyl−N−O points parallel to the plane of CB[7] and perpendicular to the plane of CB[8] (pointing toward the annulus). This difference in the orientation of DTBN upon inclusion in CB[7] and CB[8] is meant to minimize the repulsive forces exhibited by the methyl group with the CB ring system. Figure 2 shows the diameters of DTBN parallel and perpendicular to the orientation of the N−O moiety, and the difference is 3.0 Å. The larger distance of the aminoxyl−O to CB−O in CB[8] compared to CB7 (3.43 vs 4.75) provides additional support for the possibility of a lower hydrophobicity for DTBN in CB[8], as suggested by the higher a_N value, 16.4 G, Figure 4.

The calculated spin density distribution on N and O atoms for DTBN are 42.1% and 55.2%, respectively. Complexation of DTBN with CB[7] and CB[8] significantly lowered the spin densities on the nitrogen and increased the spin density on the oxygen. For the DTBN:CB[7] complex the spin density on N is 29.0%; the corresponding value for the DTBN:CB[8] complex is 25.4%. While the calculated spin density on the nitrogen atom is higher in DTBN:CB[7] compared to DTBN:CB[8], the experimental a_N for DTBN:CB[8] is higher compared to DTBN:CB[7], possibly due to the local environment: less hydrophobic or a different conformation, as suggested above. Nevertheless, our calculations provided a qualitative trend in the spin density distribution upon complexation.

Effect of Cation Addition. The effect on the ESR spectra depends on the cation concentration, as shown in Figure 6A for DTBN:CB[7]. For [NaCl] = 0.4 M, the lowest spectrum in Figure 6A, a_N is unchanged and both "out" and "in" species are

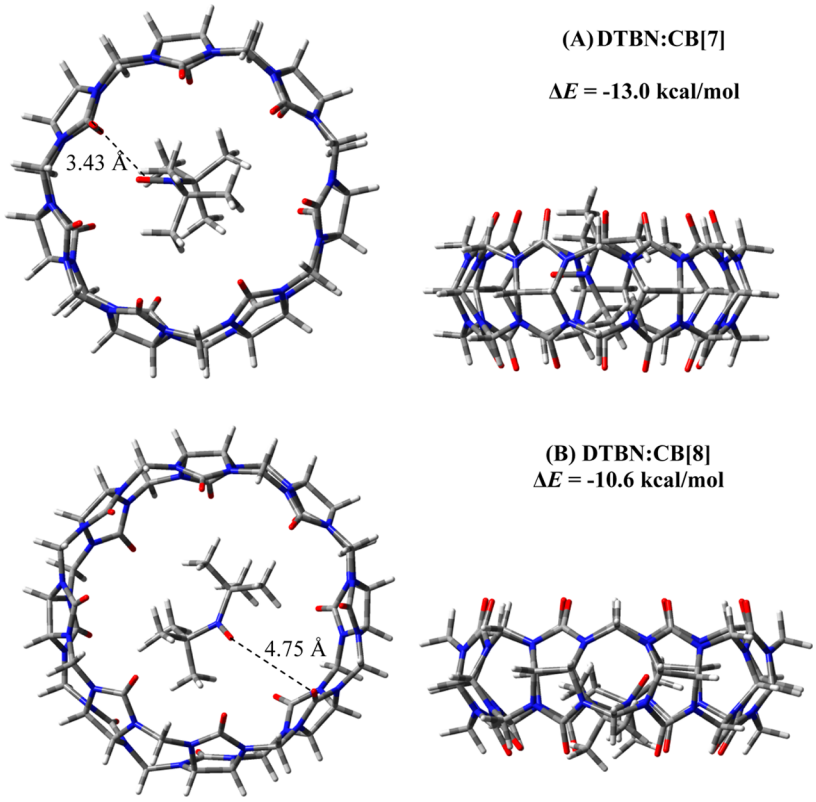

Figure 5. Optimized geometries and bottom-of-the-well energies (Δ*E*) for complexation of DTBN:CB[7] (A) and DTBN:CB[8] (B) complexes at the HF/3-21G(d) level of theory.

dx.doi.org/10.1021/jp303536m | *J. Phys. Chem. A* 2012, 116, 8475−8483

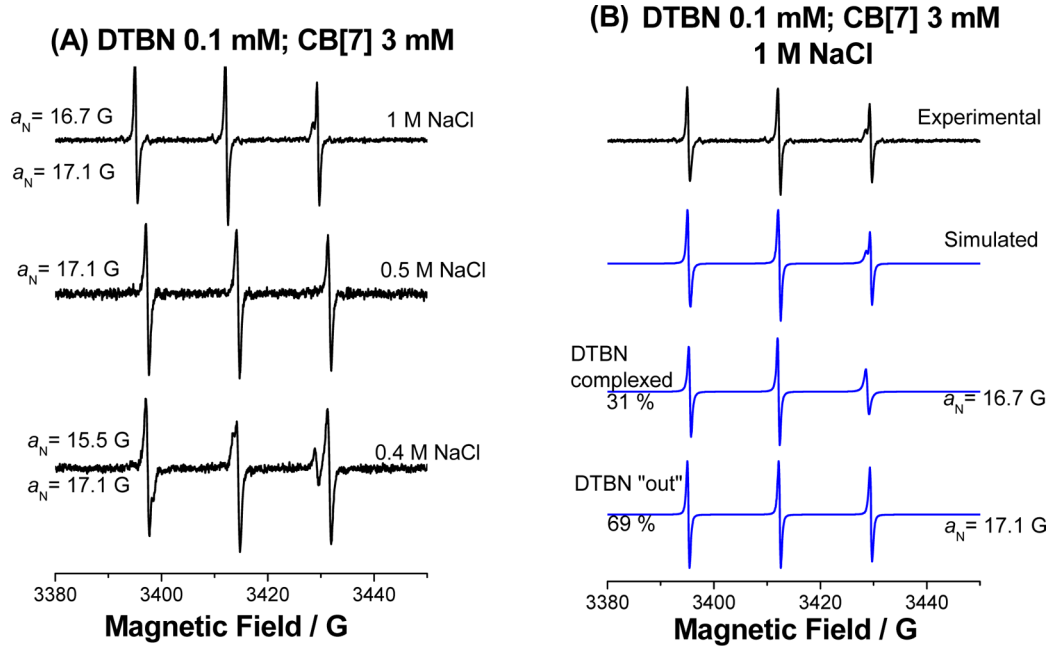

Figure 6. Effect of NaCl addition: (A) ESR spectra at 300 K of DTBN in the presence of 3 mM CB[7] and the indicated concentrations of NaCl. (B) Experimental and simulated ESR spectra for 0.1 mM DTBN in the presence of 3 mM CB[7] and 1 M NaCl. Note the higher a_N value of in DTBN (16.7 G) and its lower relative intensity compared to values given in Figure 3B (15.5 G, and 31% compared to 81%).

detected, with a_N values identical to those measured in the absence of the cations; however, the relative intensity of the "in" form, deduced from simulation of the ESR spectrum, decreased to 25%. For [NaCl] = 0.5 M only the "out" form was detected, and for [NaCl] = 1 M a new triplet appeared, with a_N = 16.7 G; simulation of the ESR spectrum, Figure 6B, indicated that DTBN "out" is still the major component, with relative intensity 69%. The line widths of the additional component, in particular the broader high-field signal, suggest a lower rate of rotational motion for this complexed DTBN. The a_N value is 16.7 G, intermediate between the values in water (17.1 G) and the "in" value, 15.5 G, most likely a result of the proximity to the polar component, NaCl.

Similar results were reported for DTBN included in Y zeolites after ion exchange with alkali-metali ions.[35] The nitroxide group of DTBN can act as a Lewis base and coordinate to an electron pair acceptor, leading to a redistribution in the N−O electron system toward the oxygen atom and increased *spin density* at the nitrogen atom which is reflected in the increase of the a_N compared to aqueous media. We assign the complexed DTBN to the formation of a DTBN:cation:CB[7] complex, similar to results published for TEMPO.[19a] This assignment is supported by both the broader line widths and the a_N value.

No effect of NaCl addition was detected in the DTBN:CB[8] system. This result can be understood by the larger distance between DTBN inside the larger host and the salt located near the host rim.

Association Constants of DTBN:CB[7]. The association constants, K_a, as a function of CB[7] concentration can be calculated from the relative intensities of the "in" and "out" species and based on the reasonable assumption that the concentration of CB[7] is higher than that of the nitroxides.[36] For these conditions

$$K_a = r_1/(r_0[\mathrm{CB}]) \quad (1)$$

In eq 1 r_1 is the concentration of the "in" species and r_0 is the concentration of the "out" species, which are presented in Tables S1−S4 in the Suporting Information. The K_a values are plotted in Figure 7 for DTBN at pH 3.2, 7 and 10 and also for the complex with Na ions in the presence of 1 M NaCl (see Table 1).

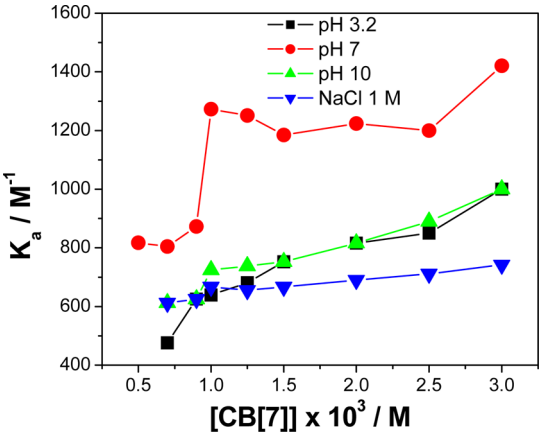

Figure 7. Association constant K_a at 300 K of DTBN as a function of CB[7] concentration and pH values. K_a values for the tricomponent complex formed in the presence of 1 M NaCl are also presented.

We note that the association constants for DTBN in CB[7] are similar to values for DTBN in β-CD,[18a] where values in the range 700−1200 M^{-1} were reported. In addition, we note that the pH value is important for determining the complexation strength, as K_a values are higher for the same concentrations of CB[7] and DTBN (kept constant) at pH 7 compared with pH 3.2 or 10. The association constant is slightly lower for the DTBN:cation:CB[7] complex formed in the presence of 1 M NaCl, but the values are high enough to indicate a good stability of these complexes.

dx.doi.org/10.1021/jp303536m | J. Phys. Chem. A 2012, 116, 8475−8483

Table 1. Association Constant K_a as a Function of pH and NaCl Concentration for DTBN at the Indicated CB[7] Concentrations

	K_a (M^{-1})			
[CB[7]] × 10^3 M	pH = 3.2	pH = 7	pH = 10	1 M NaCl
0.1	–	–	–	–
0.5	–	817	–	–
0.7	476	804	612	612
0.9	625	873	625	625
1.0	639	1273	724	667
1.25	681	1251	738	655
1.50	752	1185	752	667
2.00	816	1224	816	690
2.50	850	1200	890	711
3.00	1000	1421	1000	742

2. Complexation Between Spin Adducts and CBs. *The DMPO/OH Adduct.* The interaction between spin adducts and CB[7] has not been reported in the literature. We examined the effect of CB[7] on the spin adducts of the hydroxyl radical, DMPO/OH, and of the ·CH_2COOH radical, MNP/CH_2COOH, and the results were compared with those previously published for these adducts in the presence of β-CD.[18]

Complexation between DMPO/OH and CB[7] does not lead to measurable effects on the hyperfine splittings and on the ESR line widths of the adduct, suggesting that the N−O group is *outside* the host cavity, as also reported for this adduct in β-CD. However, a slight increase of the stability of DMPO/OH adduct was observed, as shown in Figure 8A, which presents the adduct intensity during UV irradiation and the decay after the irradiation was stopped. The intensity of the adduct is higher by a factor of 2 in the presence of 3 mM CB[7]. This effect is weaker than in the case of β-CD, where a fivefold increase was observed.[18] The half-life time of DMPO/OH, $\tau_{1/2}$, determined at the half-maximum intensity of the signal marked with red arrow in the inset of Figure 8A, is presented in Figure 8B. Encapsulation of the DMPO/OH adducts leads to an maximum increase of their half-life from 680 s in the absence of CB[7] to ≈800 s, much less than the 1500 s value reported for β-CD.[18]

No ESR signals of DMPO/OH in CB[8] were detected. More experiments are needed in order to understand this result. It is possible that the spin trap, DMPO, is preferentially complexed by CB[8]. In support of this idea, computational studies showed more favorable inclusion of DMPO in CB[8] than in CB[7]: The calculated bottom-of-the-well energy for the formation of DMPO:CB[8] is −29.2 kcal/mol compared to −19.0 kcal/mol for DMPO:CB[7], indicating that inclusion of DMPO in CB[8] could be one of the factors for the nonobservance of ESR signal: due to its encapsulation in CB[8], the spin trap is less available for scavenging the hydroxyl radical.

Optimized structures of complexes of DMPO/OH with CB[7] and CB[8] are shown in Figure 9. Intermolecular H-bonding interactions are evident for both complexes, and stronger H-bond interaction was observed with CB[7] compared to CB[8], with N−O···N bond distances of 2.07 and 2.66 Å, resepctively. The longer H-bond distance in CB[8] is due to its larger cavity size, which enables a less dynamically restricted DMPO/OH. The thermodynamics of DMPO/OH complexation with CB[7] and CB[8] are exoergic with bottom-of-the-well energies of −18.3 and −16.9 kcal/mol, respectively. The strong intermolecular H-bond interaction between CB[7] and DMPO/OH translates into more favorable energetics of complexation compared to the complexation of CBs with DTBN.

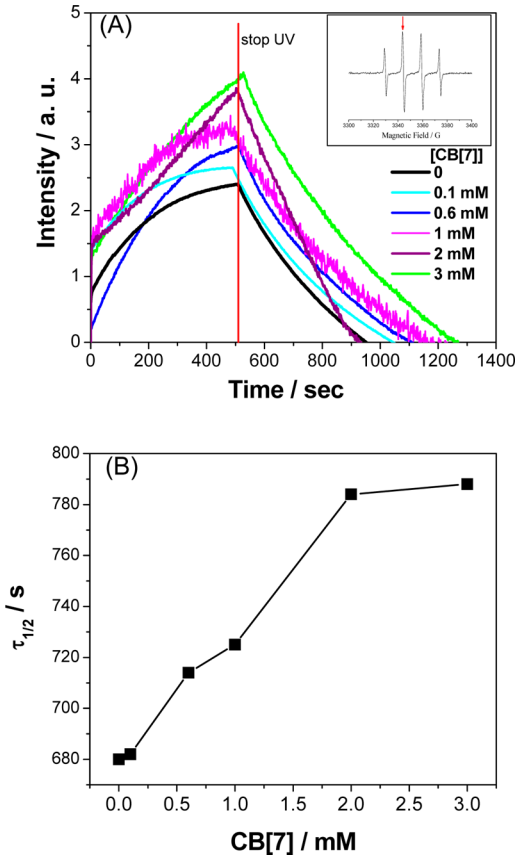

Figure 8. (A) Generation of the DMPO/OH adduct and its decay at 300 K in the absence and in the presence of the indicated CB[7] concentrations, in the range 0.1−3 mM. The red arrow in the inset points to the signal whose intensity was monitored in the time scan. (B) Half-life of the DMPO/OH adduct as a function of CB[7] concentration, determined after stopping the UV irradiation at the half-maximum intensity of the signal marked with the red line in the inset in (A). The straight lines between points are guides to the eye.

For DMPO/OH, the predicted spin densities on the N and O atoms are 38.4% and 57.8%, while the complexation of DMPO/OH with CB[7] and CB[8] lowered the spin density distribution on N, which is 20.7% in DMPO/OH:CB[7] and 27.3% in DMPO/OH:CB[8]. The greater effect of CB[7] on the spin density distribution of DMPO/OH (compared to CB[8]) may be due to the strong intermolecular interaction. However, although our predicted spin density data could explain the lower a_N measured for CB-complexed DTBN compared to that in the absence of CB, this study cannot explain why there was no change in the a_N measured by ESR for CB[7]:DMPO/OH, probably due to the incomplete inclusion of DMPO/OH in the host. Attempts to optimize DMPO/OH:CB[7] structures with the N−O moiety pointing toward the annulus always led to a DMPO/OH conformation with the N−O orientation parallel to the CB[7] annulus.

The MNP/CH_2COOH Adduct. As indicated in Figure 10A, the attack of hydroxyl radicals on acetic acid leads to formation of the $^{\bullet}CH_2COOH$ radical; the corresponding MNP adduct has a_N = 15.4 G and a_H = 8.3 G (2H) at pH = 7.[18a] The

dx.doi.org/10.1021/jp303536m | J. Phys. Chem. A 2012, 116, 8475−8483

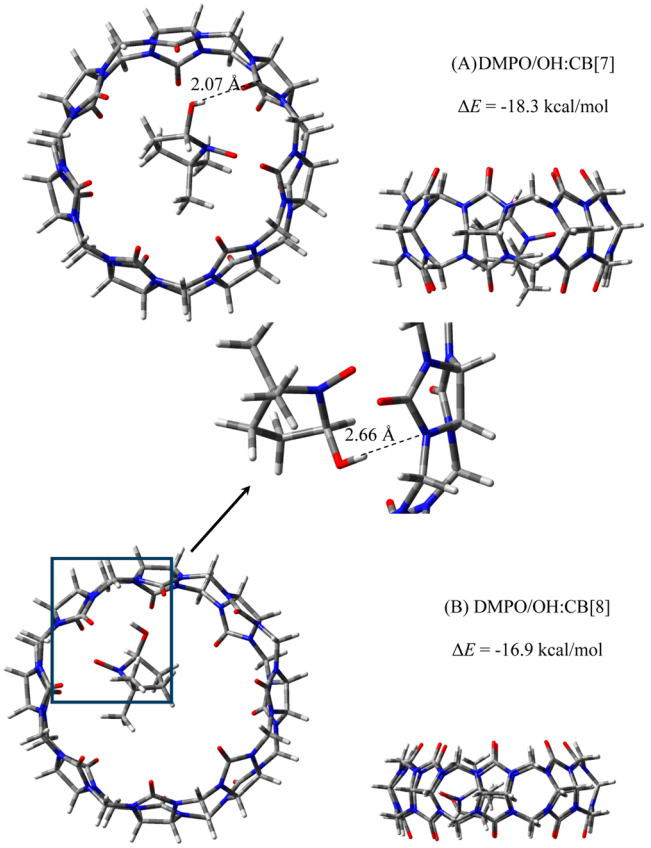

Figure 9. Optimized geometries and bottom-of-the-well energies (ΔE) of complexation for DMPO/OH:CB[7] (A) and DMPO/OH:CB[8] (B) at the HF/3-21G(d) level of theory.

presence of DTBN, with a dominant relative intensity of 85%, is also detected. The effect of CB[7] addition is shown in Figure 10B; even a small CB[7] concentration (0.1 mM) leads to the detection of a new MNP/CH_2COOH adduct with a_N = 16.2 G and a_H = 8.5 G and of the DTBN radical (with a_N = 17.1 G, as reported in aqueous media).[18] For the adduct, the increase of a_N (by 0.8 G) and a_H (by 0.2 G) can be explained by the formation of a tricomponent complex between the MNP adduct, the Na^+ cations added for pH control, and CB[7], as also reported above for DTBN. Due to the adduct interaction with CB[7], an increase of its relative intensity, from 15% in the absence to 39% in the presence of CB[7], can be seen in Figure 10B. For DTBN the a_N value is slightly higher than in the absence of CB[7] (17.1 vs 16.8 G), most likely because CB[7] reduces the interaction between the acetic acid and DTBN.[18a] In contrast to the results presented in ref 18a, no measurable increase of the lifetime of the MNP/CH_2COOH adduct was observed.

CONCLUSIONS

ESR spectroscopy combined with DFT calculations can bring new insights into the formation of supramolecular complexes of guest molecules with CBs as hosts. Using DTBN as the guest nitroxide, we have demonstrated that size incompatibility is responsible for the lack of complexation of DTBN and CB[6]. In the case of CB[7], the a_N value of the "in" form is lower by 1.6 G compared to the "out" value (15.5 G compared to 17.1 G). The intensity of in species increases with CB[7] concentration, and this trend is independent of the pH value. The interaction between DTBN and CB[7] is strong, and DFT calculations suggest that DTBN is orientated parallel to the plane of CB[7].

The presence of alkali metal cations (added as NaCl) in high concentrations results in the disappearance of the "in" form and the formation of a DTBN:cation:CB[7] complex with a_N values intermediate between the "in" and "out" forms. For CB[8] only, the one form of DTBN, with a_N = 16.4 G, was detected. We have assigned this result to strong complexation of the nitroxide in the CB[8] host, also considering that no additional signals were detected, even in the presence of 1 M NaCl. DFT calculations support the idea that DTBN is a guest in both CB[7] and CB[8] and indicate that the N−O moiety of DTBN points toward the annulus.

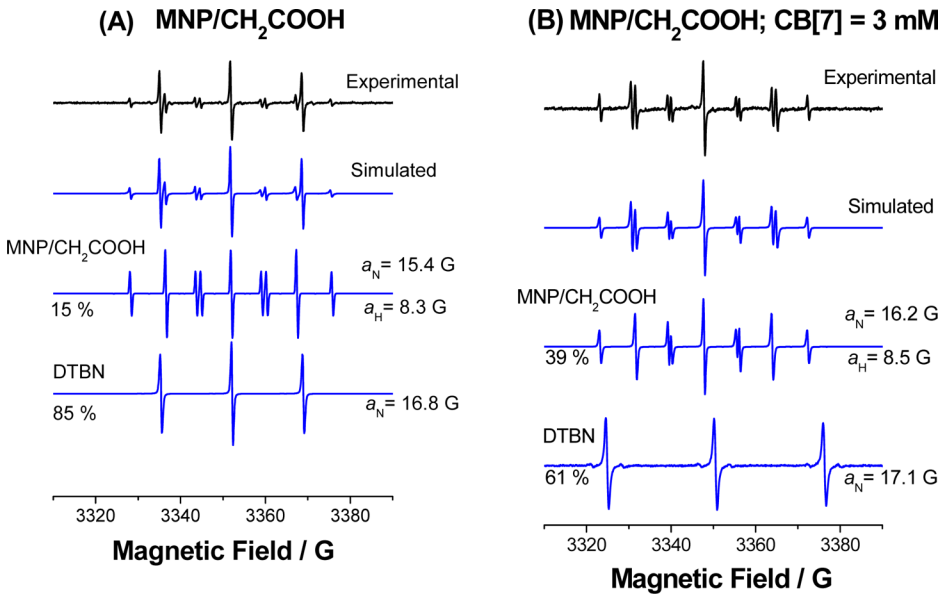

Figure 10. Experimental at 300 K and simulated ESR spectra of the MNP/CH_2COOH adduct and of DTBN radicals at pH 7, obtained in the absence of CB[7] (A) and in the presence of 3 mM CB[7] (B). Note that DTBN is also present when the MNP/CH_2COOH adduct is generated.

dx.doi.org/10.1021/jp303536m | J. Phys. Chem. A 2012, 116, 8475−8483

The complexation of CBs with spin adducts is reported here for the first time. CB[7] leads to the stabilization of the DMPO/OH adduct and a slight increase of its lifetime, but no significant changes in the a_N value or line widths were detected. DFT calculations indicate more favorable energetics of complexation for CB[7] with DMPO/OH compared with DTBN. In the case of the MNP/CH_2COOH adduct, the formation of a new adduct with higher a_N and higher intensity with increasing CB[7] concentration were observed and assigned to the formation of a three-component complex. In addition, only the out DTBN is observed in the presence of MNP adducts, suggesting the preference of CB[7] for complexation of the adducts.

The association constants for DTBN in CB[7] are similar to values for DTBN in β-CD,[18a] where values in the range 700−1200 M^{-1} were reported. The pH value is important for the complexation behavior, as K_a values are higher for the same concentrations of CB[7] and DTBN at pH 7 compared with pH 3.2 or 10. The association constant is slightly lower for the DTBN:cation:CB[7] complex formed in the presence of 1 M NaCl, but the values are high enough to indicate a good stability of these complexes.

■ ASSOCIATED CONTENT

Supporting Information

Association constants and relative intensities of the in and out DTBN in CB[7] for pH = 3.2, 7, and 10 and for experiments performed in the presence of 1 M NaCl (Figures S1−S4). This material is available free of charge via the Internet at http://pubs.acs.org.

■ AUTHOR INFORMATION

Corresponding Author

*Telephone: 1-313-993-1012. Fax: 1-313-993-1144. E-mail: schlicks@udmercy.edu.

Notes

The authors declare no competing financial interest.

‡On leave from the Institute of Macromolecular Chemistry "Petru Poni", 41A Grigore Ghica Voda, Iassy 74048, Romania.

■ ACKNOWLEDGMENTS

This research was supported by grants from the Polymers Program of the National Science Foundation.

■ REFERENCES

(1) Lee, J. W.; Samal, S.; Selvapalam, N.; Kim, H. J.; Kim, K. *Acc. Chem. Res.* **2003**, *36*, 621−630.
(2) Lagona, J.; Mukhopadhyay, P.; Chakrabarti, S.; Isaacs, L. *Angew. Chem., Int. Ed.* **2005**, *44*, 4844−4870.
(3) Choudhury, S. D.; Mohanty, J.; Upadhyaya, H. P.; Bhasikuttan, A. C.; Haridas, P. *J. Phys. Chem. B* **2009**, *113*, 1891−1898.
(4) Flinn, A.; Hough, G. C.; Stoddart, J. F.; Williams, D. J. *Angew. Chem., Int. Ed. Engl.* **1992**, *57* (11), 1475−147.
(5) Werner, N.; Scherman, O. A. *Isr. J. Chem.* **2011**, *51*, 492−494.
(6) Kim, K.; Selvapalam, N.; Oh, D. H. *J. Inclusion Phenom. Macrocyc. Chem.* **2004**, *50*, 31−36.
(7) Kim, J.; Jung, I.-S.; Kim, S.-Y.; Lee, E.; Kang, J.-K.; Sakamoto, S.; Yamaguchi, K.; Kim, K. *J. Am. Chem. Soc.* **2000**, *122*, 540−541.
(8) Szejtli, J. *Chem. Rev.* **1998**, *98*, 1743−1754.
(9) Leclercq, L.; Noujeim, N.; Sanon, S. H.; Schmitzer, A. R. *J. Phys. Chem. B* **2008**, *112*, 14176−14184.
(10) Da Silva, J. P.; Jayaraj, N.; Jockusch, S.; Turro, N. J.; Ramamurthy, V. *Org. Lett.* **2011**, *13* (9), 2410−2413.
(11) Rekharsky, M. V.; Mori, T.; Yang, C.; Ko, Y. H.; Selvapalam, N.; Kim, H.; Sobransingh, D.; Kaifer, A. E.; Liu, S.; Isaacs, L.; et al. *Proc. Natl. Acad. Sci. U.S.A.* **2007**, *104*, 20737−20742.
(12) Zhang, J.; Coulston, R. J.; Jones, S. T.; Geng, J.; Scherman, O. A.; Abell, C. *Science* **2012**, *335*, 690−694.
(13) Marquez, C.; Hudgins, R. H.; Nau, W. M. *J. Am. Chem. Soc.* **2004**, *126*, 5806−5816.
(14) Philip, D; Stoddart, J. F. *Angew. Chem., Int. Ed. Engl.* **1996**, *35*, 1154−1196.
(15) Nau, W. M.; Wang, X. *ChemPhysChem* **2002**, *3*, 393−398.
(16) Schneider, H. J.; Hacket, F.; Rudiger, V. *Chem. Rev.* **1998**, *9*, 1755−1785.
(17) Franchi, P.; Lucarini, M.; Pedulli, G. F. *Curr. Org. Chem.* **2004**, *8*, 1831−1849.
(18) (a) Spulber, M.; Schlick, S. *J. Phys. Chem. A* **2010**, *114*, 6217−6225. (b) Spulber, M.; Schlick, S. *J. Phys. Chem. B* **2011**, *115*, 12415−12421.
(19) (a) Mezzina, E.; Cruciani, F.; Pedulli, G. F.; Lucarini, M. *Chem.—Eur. J.* **2007**, *13*, 7223−7233. (b) Mileo, E.; Mezzina, E.; Grepioni, F.; Pedulli, G. F.; Lucarini, M. *Chem.—Eur. J.* **2009**, *15*, 7859−7862.
(20) Bardelang, D.; Banaszak, K.; Karoui, H.; Rockenbauer, A.; Waite, M.; Udachin, K.; Ripmeester, J. A.; Ratcliffe, C. I.; Ouari, O.; Tordo, P. *J. Am. Chem. Soc.* **2009**, *131*, 5402−5404.
(21) (a) Jayaraj, N.; Porel, M.; Ottaviani, M. F.; Maddipatla, M. V. S. N; Modelli, A.; DaSilva, J. P.; Bhogala, R. B.; Captain, B.; Jockusch, S.; Turro, N. J.; et al. *Langmuir* **2009**, *25*, 13820−13832. (b) Yi, S.; Captain, B.; Ottaviani, M. F.; Kaifer, A. E. *Langmuir* **2011**, *27*, 5624−5632.
(22) (a) Han, Y.; Tuccio, B.; Lauricella, R.; Villamena, F. A. *J. Org. Chem. A* **2008**, *73*, 7108−7117. (b) Han, Y.; Liu, Y.; Rockenbauer, A.; Zweier, J. L.; Durand, G.; Villamena, F. A. *J. Org. Chem. A* **2009**, *74*, 5369−5380.
(23) (a) Gobre, V. V.; Pinjari, R. V.; Gejji, S. P. *J. Phys. Chem. A* **2010**, *114*, 4464−4470. (b) Pinjari, R. V.; Gejji, S.P. *J. Phys. Chem. A* **2008**, *112*, 12679−12686. (c) Hang, C.; Li, C.-R.; Xue, S.-F.; Zhu, T.; Zhu, Q.-J.; Wei, G. *Org. Biomol. Chem.* **2011**, *9*, 1041−1046.
(24) http://www.niehs.nih.gov/research/resources/software/tools/index.cfm.
(25) Frisch, M. J.; Trucks, G. W.; Schlegel, H. B.; Scuseria, G. E.; Robb, M. A.; Cheeseman, J. R.; Montgomery, J. A., Jr.; Vreven, T.; Kudin, K. N.; Burant, J. C. et al. *Gaussian 03*; Gaussian, Inc.: Pittsburgh, PA, 2003.
(26) Labanowski, J.; Andzelm, J. *Density Functional Methods in Chemistry*; Springer: New York, 1991.
(27) Scott, A. P.; Radom, L. *J. Phys. Chem.* **1996**, *100* (41), 16502−16513.
(28) Reed, A. E.; Curtiss, L. A.; Weinhold, F. *Chem. Rev.* **1988**, *88* (6), 899−926.
(29) Eastman, M. P.; Brainard, J. R.; Stewart, D.; Anderson, G.; Lloyd, W. D. *Macromolecules* **1989**, *22*, 3888−3892.
(30) Suvitha, A.; Venkataramanan, N. S.; Mizuseki, H.; Kawazoe, Y.; Ohuchi, N. *J. Inclusion Phenom. Macrocycl. Chem.* **2010**, *66*, 213−218.
(31) Baur, M. E.; Bales, B. L. *Chem. Phys. Lett.* **1970**, *7* (3), 341−344.
(32) Camargos, H. S.; Silva, A. H. M.; Anjos, J. L. V.; Alonso, A. *Lipids* **2010**, *45*, 419−427.
(33) Janzen, E. G. In *Topics in Stereochemistry*; Allinger, L. L., Eliel, E. L., Eds.; Wiley-Interscience: New York, 1971; Vol. *6*, pp 186−199.
(34) Franchi, P.; Casati, C.; Mezzina, E.; Lucarini, M. *Org. Biomol. Chem.* **2011**, *9*, 6396−6401.
(35) Gutjahr, M.; Poppl, A.; Bohlmann, W.; Bottcher, R. *Colloids Surf., A* **2001**, *189*, 93−101.
(36) Kotake, Y.; Janzen, E. G. *J. Am. Chem. Soc.* **1989**, *111*, 5138−5140.